MEASUREMENTS WITH HIGH SPATIAL RESOLUTION OF CHLOROPHYLL-A, CDOM AND TOTAL SUSPENDED MATTER IN COASTAL ZONES AND INLAND WATER BODIES BY THE PORTABLE UFL LIDAR

Vadim Pelevin[1] (pelevin@ocean.ru), Peter Zavialov[1], Boris Konovalov[1], András Zlinszky[2], Stephanie Palmer[2], Viktor Toth[2], Igor Goncharenko[1], Lisa Khymchenko[1], Varvara Osokina[1]

1: Shirshov Institute of Oceanology of the Russian Academy of Sciences, Moscow, Russia
2: Balaton Limnological Research Institute of the Hungarian Academy of Sciences, Tihany, Hungary

This paper presents certain results of remote sensing of the seas and inland waters, obtained using a portable Laser Induced Fluorescence (LIF) LiDAR in the expeditions of the Shirshov Institute of Oceanology, Russian Academy of Sciences in recent years.

The ultra-violet fluorescence lidars (UFL) portable series used in these studies were developed at the Shirshov Institute in 2001-2009. It can be used for chromophoric dissolved organic matter (CDOM), organic pollutants, chlorophyll-a (chl*a*), and total suspended matter (TSM) concentrations measurements at high spatial resolution (up to 1 m). TSM measurements are conducted due to backscattered laser radiation. Suspended matter concentration we consider as a proportional value to backward scattering coefficient of the water medium at laser wavelength. The data have been gathered with 2Hz rate from any size research vessels continuously during daytime while the ship was travelling - one simultaneous measurement of all parameters per each laser pulse. In particular, near some river mouths the lidar measurements were carried out from inflatable boats for the purpose of gathering extra-high spatial resolution and near-shore fluorescence data. All point locations were measured by GPS and maps were created by interpolation using GIS software. Main parameters of lidar UFL-9 are presented and some methodology issues are discussed in the paper.

The lidar data were calibrated against those obtained in situ through water sampling and then converted from the optical units into the mass concentrations of the above mentioned constituents.

Spatial and temporal variability (patchiness) of CDOM, chlorophyll-a and TSM in lakes and open water bodies can often serve as a proxy for circulation patterns and characterize the state of shelf ecosystems, in particular, those in estuarine areas and regions exposed to anthropogenic impacts. The small-scale variability spanning in the range of only a few meters to first hundreds of meters is perhaps the least well understood because of lack of instruments and methods capable of achieving such a resolution.

1. Introduction

LIF LiDAR sensing method is widely used for the study of coastal seas and open water since the 1970s (e.g. Farmer et al. 1979, Abramov et al. 1977, Hoge and Swift 1981, Barbini et al. 1999). Different shipborne and airborne fluorescence LiDARs are developed and successfully used in marine researches (e.g. Babichenko et al. 2004, Aibulatov et al. 2008, Utkin et al. 2011). Because of the high cost and bulkiness of the equipment, it is still quite exotic and not included in the broad practice of oceanographic and limnological researches.

In this paper, we want to describe briefly the Ultraviolet Fluorescent LiDARs (UFL series) developed in the Shirshov Institute and enumerate the features and benefits of this technique. In short, we can list the main advantages and differences from analogs:

- Small size and weight, one can use it with any ship, starting from oceanic research vessels to the smallest inflatable boats. This feature allows applying it in the seas and in lakes and rivers also.

- The ability to measure the concentration of not only the CDOM and chlorophyll *a*, but also the total suspended matter;

- High sensitivity and independence from solar illumination level of the sea surface, UFL is able to receive signals of fluorescence in ultra-oligotrophic waters in the afternoon when the sun is high, even when working on the solar path;

- Automatic mode and bind to the GPS-coordinates, PC-controlled, all-weather use.

Since 2002, LIDARs UFL-series have been successfully used for scientific and environmental investigations in more than 30 expeditions in salty and fresh waters in open and inland water bodies (the Black, Baltic, North, Mediterranean, Barents, Kara, Aral, China Seas, the Atlantic Ocean, the Lakes Balaton and Issyk-Kul).

It should be mentioned that the sensitivity of the LiDAR technique is higher compared to a flow-through or immersion fluorometers since the powerful laser ray penetrates to a greater depth in the water column, causing the fluorescence of the constituents (the thickness of the water layer varies 0.5-10 meters according of water turbidity for UFL-9). Furthermore, LiDAR works through the water surface, and even the thin surface layer or film contributes to the fluorescence response. This fact is important for the control of organic pollution (including oil films), and for researches in highly stratified coastal areas under the influence of river runoff. When using flow-through systems onboard marine research vessels it is not possible to carry out continuous sampling of sea water from the depths less than 2-3 meters because of the inevitable presence of the waves on the sea surface.

The paper presents the results of the UFL-9 LiDAR measurements in two expeditions - in the Kara Sea in 2011 and in the Lake Balaton in 2012, as an example of the UFL’s application in oligotrophic saltwater basin onboard oceanic research vessel and in shallow eutrophic freshwater lake onboard the high-speed small motorboat.

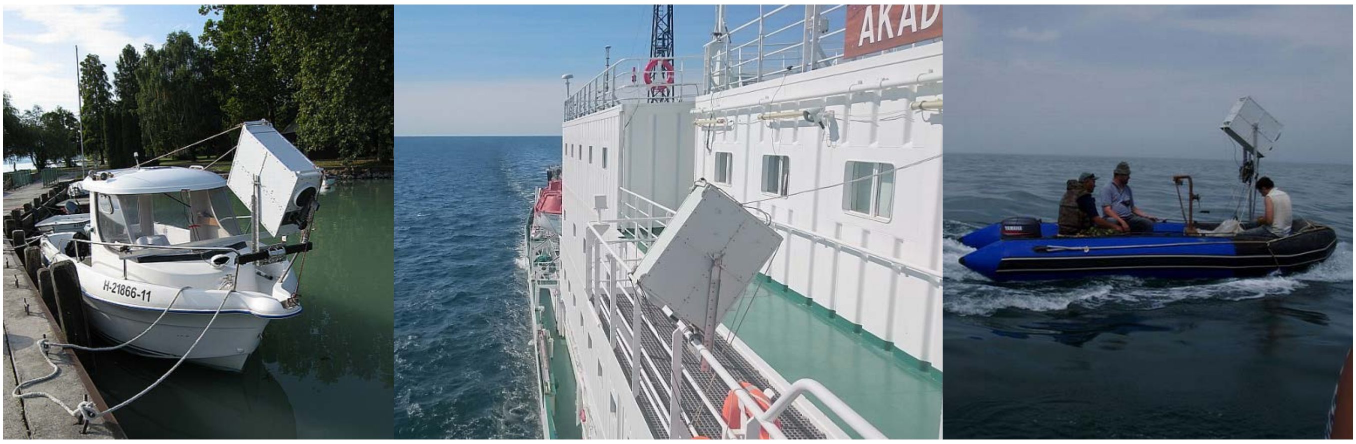

2. Materials and Methods

2.1. Basis of the Method

Laser pulse of energy $\mathbf{N_0}$ (λ=355 nm) is sounding the sea surface in the direction closely to vertical line. To the depth **z** it is coming energy equals to

$N = N_0 \cdot \exp(- K_{d355}\, z)$,

where K_{d355} - vertical attenuation coefficient.

Despite the fact that the probe is held by narrow light beam, the vertical attenuation coefficient K_d should be used, specific for a wide beam of sunlight. This is because we consider the energy pulse has reached **z** horizon, regardless of blur of the beam in a direction transverse to the beam axis. The angular aperture of the UFL receiver system is much bigger than the angular divergence of the laser beam, including taking into account its cross blur. All outgoing photons reached the depth **z** are involved in the formation of the backscatter signal, fluorescence signal, etc. Therefore, taking into account the attenuation of light in the vertical direction should be used the vertical attenuation coefficient K_d which is introduced for the solar radiation flux.

A layer of water with depth **dz** scatters back radiation of energy that equals to

$dN_{355} = N_0 \cdot \exp(- K_{d355}\, z) \cdot \beta_{355}\, dz$

where $\boldsymbol{\beta_{355}}$ – backward scattering coefficient by elementary volume of water at λ=355 nm.

Scattered back (BS) by elementary layer and reached to the surface energy equals to

$dN_{BS} = N_0 \cdot \exp(-2\, K_{d355}\, z) \cdot \beta_{355}\, dz$.

Full energy scattered by semi-infinite sea medium in the direction back to the laser beam follows: (after integration by z):

$N_{BS} = N_0 \cdot \beta_{355} \cdot 1/(2\ K_{d355})$.

Portion of energy having hit into the photo detector considered by introduction of multiplier **G**:

$N_{BS} = N_0 \cdot \beta_{355} \cdot G \cdot 1/(2\ K_{d355})$.

Here **G** – «geometrical» factor, it is dependent from the altitude of the LiDAR above the sea surface, slope angle of laser axle to the surface, hade of beam on the border "water-air" and etc.

By analogy, we can write that the energy of the pulse of Raman scattering that reached the receiver (i.e. N_{RS}) equals:

$N_{RS} = N_0 \cdot \gamma_{RS} \cdot G \cdot 1/(K_{d404} + K_{d355})$,

where $\boldsymbol{\gamma_{RS}}$ – a constant, which is defined by Raman scattering of water medium.

Flux of radiation being made by fluorescence of colored dissolved organic matter and reaching the photo detector is calculated similarly, but instead of $\boldsymbol{\beta_{355}}$ it is substituted the value of absorption coefficient by organic matter $\mathbf{a_{DOM,355}}$, multiplied on $\boldsymbol{\delta_{355\to\lambda}}$ - a coefficient that considers transport of absorbed energy to spectral zone λ and fluorescence yield.

The practice has shown that for the estimation of the CDOM concentration in upper sea layer it can be selected any spectral zone inside broad peak of fluorescence of dissolved organics. For example, a zone clipped by interference filter with wavelength of maximum transmission near 440 nm (15 nm FWHM):

$dN_{440} = N_0 \cdot \exp(-\ K_{d355}\ z) \cdot a_{DOM,355} \cdot \delta_{355\to440}\ dz$.

A contribution of the layer ***dz*** in the fluorescence flux reached the surface:

$dN_{440} = N_0 \cdot \exp(-(K_{d355} + K_{d440})z) \cdot a_{DOM,355} \cdot \delta_{355\to440}\ dz$.

Registered CDOM fluorescence:

$N_{440} = N_0 \cdot a_{DOM,355} \cdot \delta_{355\to440} \cdot G(\alpha_{355} + \alpha_{440})^{-1}$.

Chlorophyll *a* concentrations are estimated by the signal of the fluorescence near $\lambda \cong 685$nm:

$N_{685} = N_0 \cdot a_{pigm.355} \cdot \delta_{355\to685} \cdot G(K_{d355} + K_{d685})^{-1}$,

where $a_{pigm.355}$ – light absorption coefficient by phytoplankton pigments at 355 nm [m^{-1}],

$\delta_{355\to685}$ – transport factor of absorbed energy by phytoplankton pigments inside their cells to the red spectral zone $\lambda \cong 685$ nm, where this energy is highlighted.

As well we suppose that:

$a_{pigm.355} = a^{*}_{pigm.355} \cdot C_{chlA}$

where $C_{chl\ A}$ - chlorophyll concentration [mg/m^3],

$a^{*}_{pigm355}$ – specific absorption of pigments [m^{-1}].

We use the relation of amplitudes of signals N_{685}/N_{RS} for excluding N_0 and G. As a result we get the equation:

$C_{chlA} = C\,\Psi\,N_{685} / N_{RS}$,

where C – a constant,

$\Psi = (K_{d355} + K_{d685}) / (K_{d355} + K_{d404})$. Value Ψ is a function of the optical type of waters.

The concentration of total suspended matter estimation can be made on a basis of LiDAR measurements by the following way. As follows from the formulas shown above for N_{BS} and N_{RS}, quotient after their division one on another equals to β_{355}/γ_{RS} (taking into account that $2\alpha_{355} \cong (\alpha_{355} + \alpha_{404})$). We get the following equation:

$\beta_{355} = k\,N_{BS}/N_{RS}$,

where k is a calibrating coefficient.

Suspended matter concentration we suppose is proportionate to β_{355}, i.e. backward scattering coefficient of the medium at this wavelength, with the deduction of backward scattering being created by the “absolutely pure” sea water.

2.2. Ultraviolet Fluorescence LiDAR (UFL-9)

UFL-9 LiDAR was developed by the Shirshov Institute of Oceanology in 2007 (Aibulatov et al. 2008). Since 2008 it was used in several regular marine and limnological surveys, in particular on the Lake Balaton expedition in 2012 and the Kara Sea in 2011 for estimation of CDOM, chlorophyll *a* and total suspended matter. UFL takes measurements in relative (or Raman) units with sampling rate up to 2 Hz while the boat is travelling. The registration of the measured values is connected to a GPS, so all measurements are geo-tagged and can be used for interpolating maps of the measured parameters. More detailed information about UFL LiDAR and laboratory calibration experiments are previously published (Palmer et al. 2013). Investigations in open sea waters of the Atlantic Ocean are given by Koprova et al. 2010. Chinese, Black and Kara Seas UFL researches are given by Zavialov et al., 2010, 2014, 2015.

The UFL-9 measures the total suspended matter concentration in addition to chl*a* and CDOM (Aibulatov et al. 2008). It allows the simultaneous detection of water quality parameters mentioned above and can be extremely conducive not only in open sea, but also in optically complex lake waters. UFL measures near-surface concentrations optically in situ, on a travelling boat, and so is capable of a large number of widespread measurements in a short time. In addition, UFL observations could provide an accurate estimates in turbid inland waters such as Lake Balaton.

Practical applications of UFL-9 LiDAR are:

- the high spatial resolution mapping of basic water-quality parameters;
- ground truth data collecting for the proper interpretation of satellite imaging;
- express ecological control of water pollution by different organic matters, such as sewage waters, organic fertilizers, oil films, etc.;
- determining in background mode the extremum points of variability of water-quality parameters or pollution level for the water sampling or conducting a complex oceanographic measurements in the right place;
- detecting of oil products on seawater surface and estimating the oil film thickness.

Also the instrument has a high sensitivity and its functioning is independent from the level of solar illumination of the sea surface, it is able to detect signals of chl*a* fluorescence even in ultra-oligotrophic waters in sunny conditions. The main parameters of the LiDAR UFL-9 are presented in the following table.

Excitation laser wavelengths	355, 532 nm
Receiver central wavelength, transect mode	355, 404, 440, 685 nm
Additional spectral channels	385, 424, 460, 499, 532, 620, 651 nm
Bandwidth	10-15 nm FWHM
Laser pulse repetition rate	2 Hz
Laser pulse duration	6 ns
Laser pulse energy	1.5 mJ (355 nm pulse), 3 mJ (532 nm pulse)
Telescope	Kepler; adjustable length to target range 1.5–25 m
Power supply	220 V, 50 Hz, 120 W
Dimensions; weight	800 × 550 × 250 mm; 35 kg netto
Receivers	Photomultipliers
Channel filters	Four-channel beam splitter; interference filters
Telescope clear aperture	140 mm
ADC frequency	50 MHz
ADC resolution	10 bit

The returning signals from dual excitation (355, 532 nm) Nd:YAG laser pulses are detected across 11 bands on stations simultaneously with water sampling for the instrument calibration, and across 4 bands in transection mode in case of moving boat. Fluorescence intensities at 440 and 685 nm, and backscattering of the 355 nm pulse are normalized to Raman scattering at 404 nm, then calibrated to a subset of known laboratory-measured concentrations to derive CDOM, chl*a* and TSM respectively. Ranges of measured values: chl*a* - 0.01–400 mg·m^{-3}, TSM - from <0.1 to 120 g·m^{-3}, and CDOM - from 0.001–0.15 absorption m^{-1} at 440 nm.

2.3. UFL calibration

The verification of the LiDAR measurements should be performed for each water body and for each season, in order to obtain maps of the spatial distribution of water quality parameters in absolute weight units. Detected signals of fluorescence and back-scattering in Raman units depend on many factors - for chlorophyll *a* it is the species composition of phytoplankton, its phase of succession and physiological state, abiotic factors of the aquatic environment; for CDOM - its molecular composition; for mineral suspended matter - its particle size distribution.

In the Kara Sea LiDAR data were calibrated based on the results of standardized laboratory measurements of the concentrations of chlorophyll a, total organic carbon, equal to the sum of particulate and dissolved, and the mass concentration of suspended matter. We suppose, that the relatively low correlation coefficient (R^2 = 0.77) for the LiDAR measured CDOM and obtained from water samples the total organic carbon caused by the fact that the laser light is absorbed only by the colored part of the organic substance in the upper sea layer. Since the route of the ship took place in open and coastal waters under the influence of continental runoff of different origins, different types of water might contain organic substances of different molecular composition. The correlation coefficients for the chlorophyll *a* (R^2 = 0,86) and suspension (R^2 = 0,86) demonstrated satisfactory reliability of LiDAR measurements.

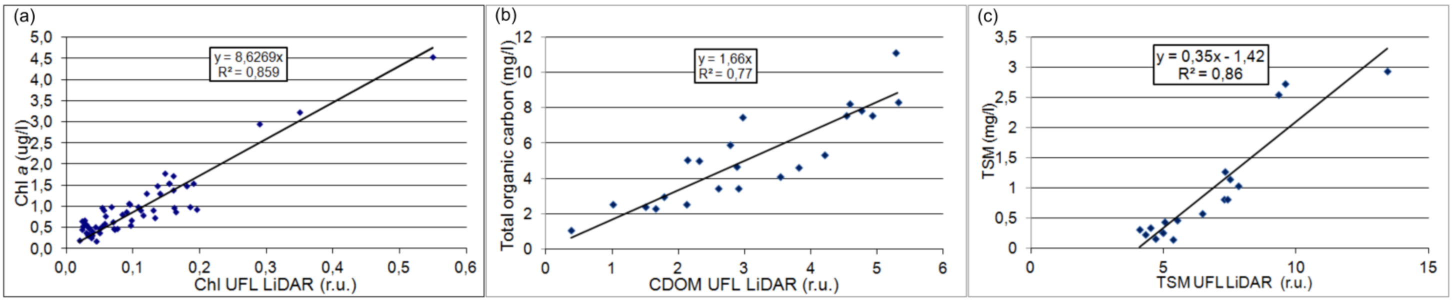

In the Balaton fieldwork the chl*a* and TSM concentrations, and CDOM absorbance of all water samples collected from water surface during the UFL field campaign were analyzed following the standard protocol of the Nutrient Cycling Laboratory of the Balaton Limnological Institute. Chl*a* concentrations were determined through spectrophotometric analysis following extraction by hot methanol and centrifugation from known volumes. TSM concentrations were determined by weight, following the drying of filtered samples of known volume on pre-dried and weighed GF/C filters (1.2 µm). CDOM was determined spectrophotometrically through absorbance measurements at 440 nm. Spectrophotometric measurements of both chl*a* and CDOM were made using a Shimadzu spectrophotometer, model UV 160A. Correlation coefficients are higher because of significant data range and the operative processing of water sampling laboratory analyses.

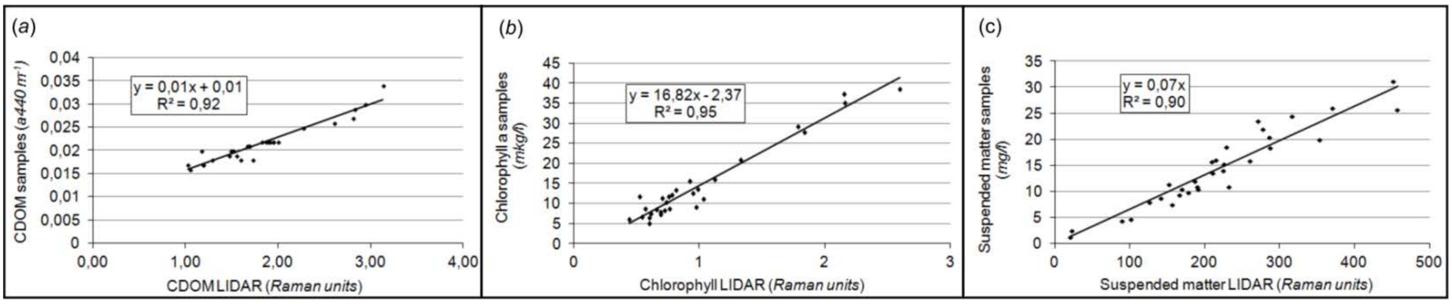

3. Water quality mapping

3.1. Kara Sea

Mesoscale and sub mesoscale variability of chlorophyll, dissolved organic matter and suspended matter in the range of tens of meters to a few kilometers, is probably the least understood due to a lack of instrumental techniques to obtain such information. Satellite data typically do not provide the required spatial resolution, and it is impossible to carry out such frequent measurements by contact methods. The measurements were made continuously while the vessel moved during 1 month, totally produced more than 1 million laser soundings. Using the results of the measurements the spatial distribution maps of bio-optical parameters were created at different scales, including the entire sea area.

Laser ray passes through the surface of the sea, so in terms of the surface layer desalination by continental runoff and increased vertical stratification, main contribution to the fluorescence makes the thin upper most fresh and rich terrigenous matter layer of water. This situation is typical for the basin of the Kara Sea, which is under the influence of powerful continental runoff of rivers Ob and Yenisei, bringing in the Kara Sea basin large masses of mineral matter, organic substances and nutrients. The Kara waters are characterized by strong frontal zones, often quite narrow (from tens and hundreds of meters to tens of centimeters), a large variety of mesoscale and sub mesoscale structures, as well as a significant distribution of river plumes on the surface of the Sea.

The red lines on the following figures consist of individual points at which the UFL measurements occurred. Bigger red dots mean the points of water sampling for the instrument calibration.

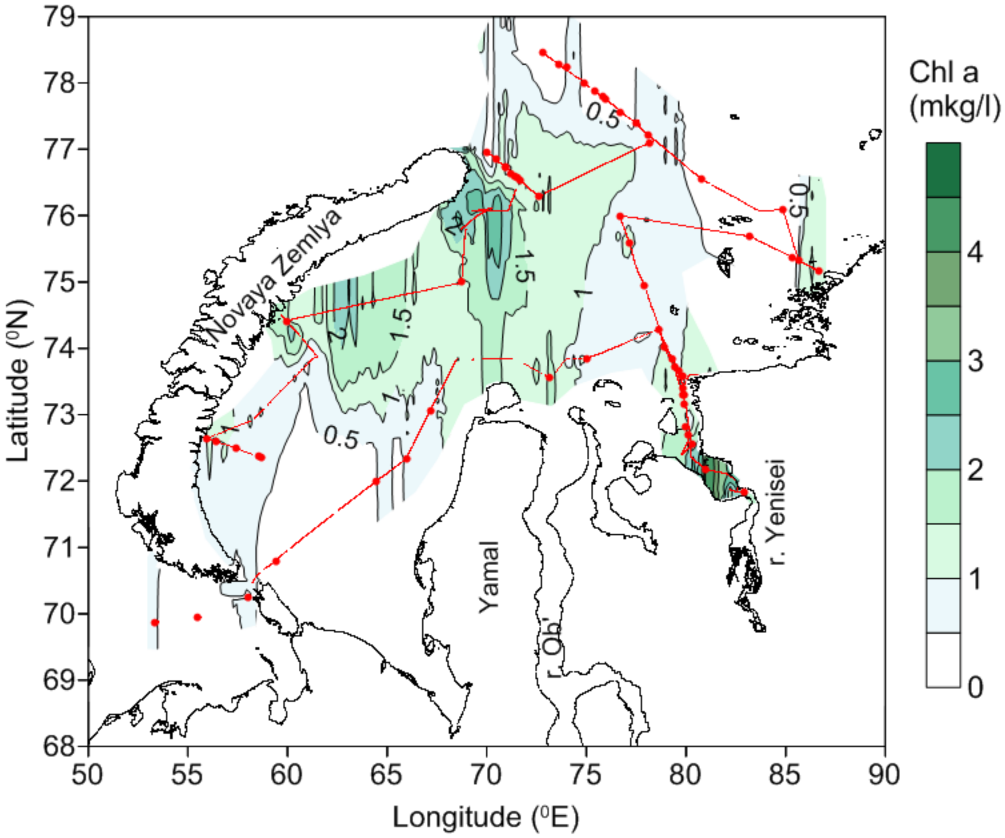

Chl a (mkg/l)
Novaya Zemlya
Yamal
r. Ob'
r. Yenisei
Latitude (⁰N)
Longitude (⁰E)

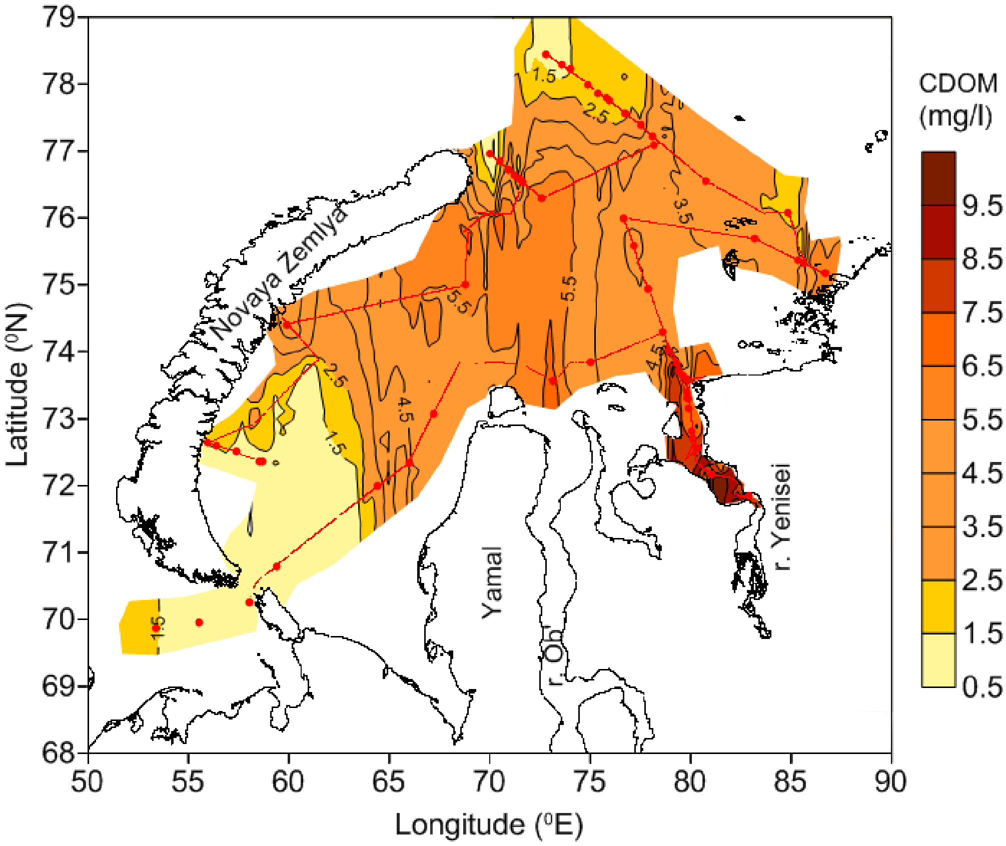

CDOM (mg/l)
Novaya Zemlya
Yamal
r. Ob'
r. Yenisei
Latitude (⁰N)
Longitude (⁰E)

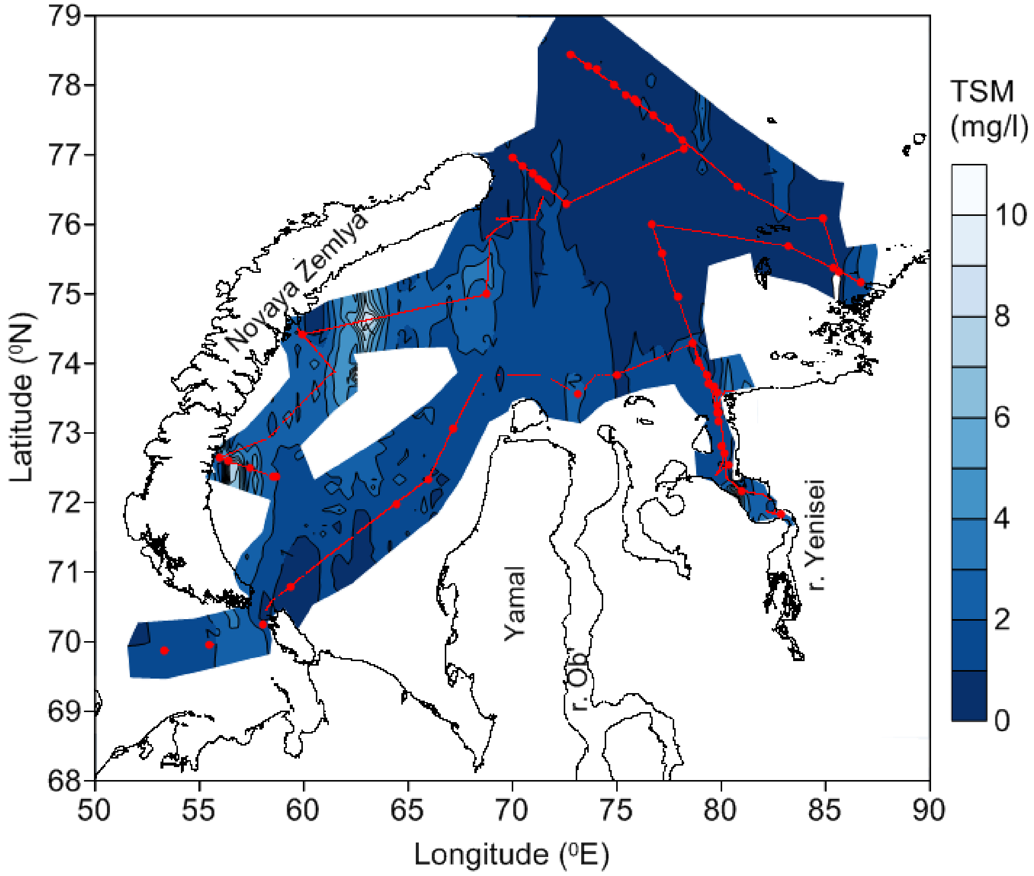

3.2. Lake Balaton

Historically the lake is eutrophic-mesotrophic, exhibiting a strong trophic gradient from SW to NE. It is considered to be, that a longitudinal trophic gradient persists in Lake Balaton with generally higher phytoplankton biomass and associated chlorophyll *a* concentrations in the southwestern-most basin (generally considered eutrophic to hypertrophic), declining to the northeastern-most basin (generally considered mesotrophic). This is related to the only major inflow into the lake, the nutrient rich Zala River, in the southwestern-most basin and the predominantly southwest to northeast circulation. As can be seen from the figures below, this prevailing view requires further observation and verification. The general southwest-northeast CDOM gradient has been found to be controlled by inflow from the Zala River, and subsequent circulation and photodegradation from southwest to northeast. TSM concentrations are mainly dependent from the wind, because of shallowness and often resuspension effects in windy conditions.

One-day measurements (07.06.2012) on the Lake Balaton, UFL is in a transect mode, registering the 3 main parameters simultaneously:

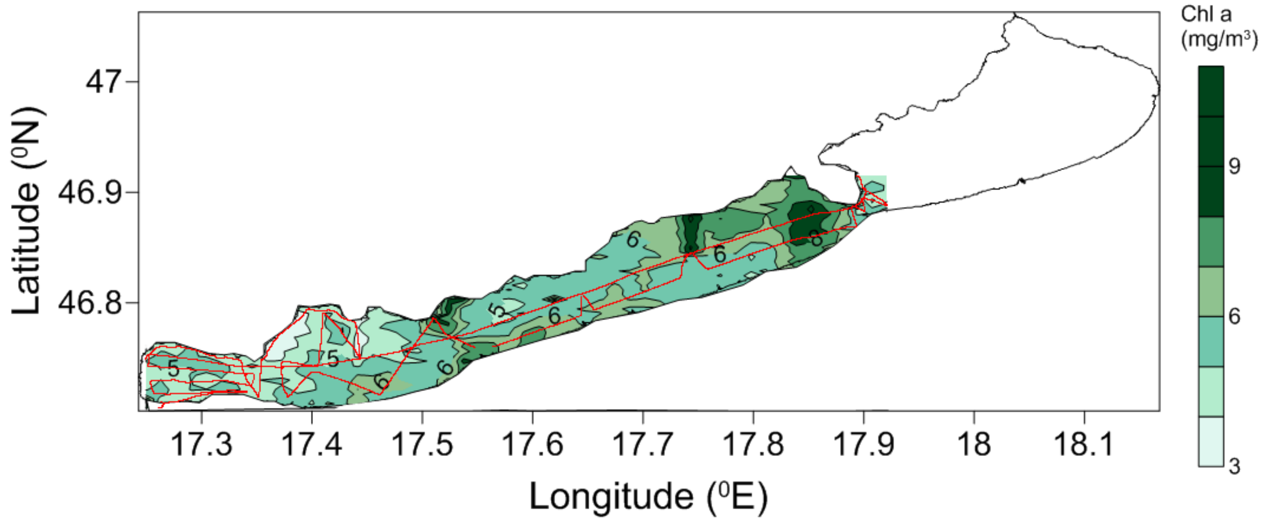

Chl a
(mg/m3)
9
6
3
47
46.9
46.8
Latitude (0N)
17.3
17.4
17.5
17.6
17.7
17.8
17.9
18
18.1
Longitude (0E)
5
6
8

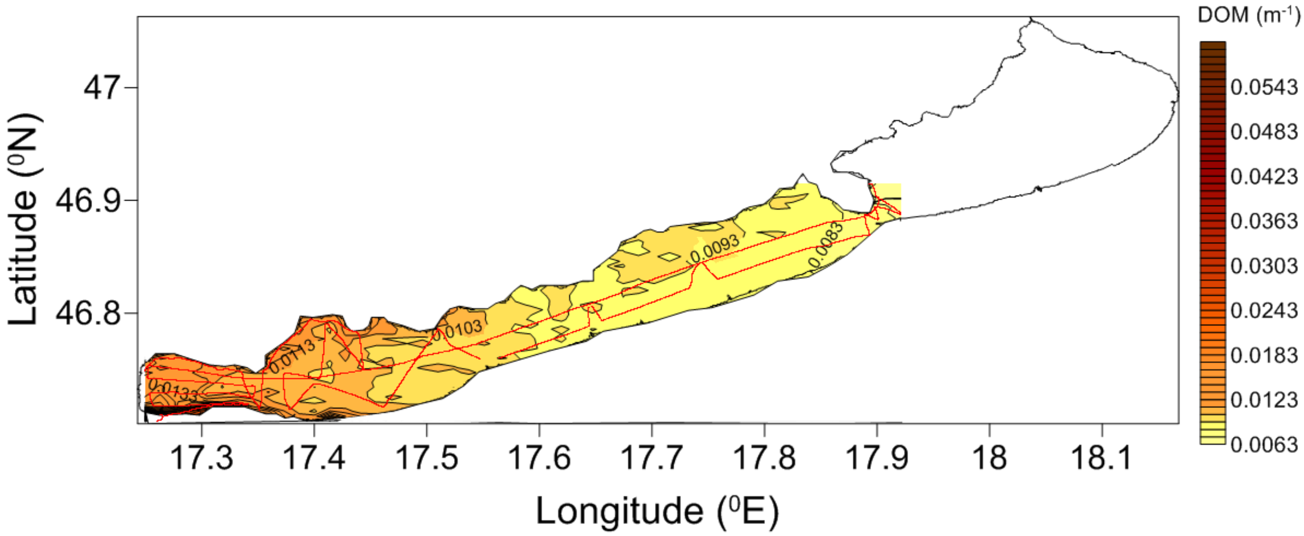

DOM (m-1)
0.0543
0.0483
0.0423
0.0363
0.0303
0.0243
0.0183
0.0123
0.0063
47
46.9
46.8
Latitude (0N)
17.3
17.4
17.5
17.6
17.7
17.8
17.9
18
18.1
Longitude (0E)
0.0093
0.0083
0.0103
0.0113
0.0133

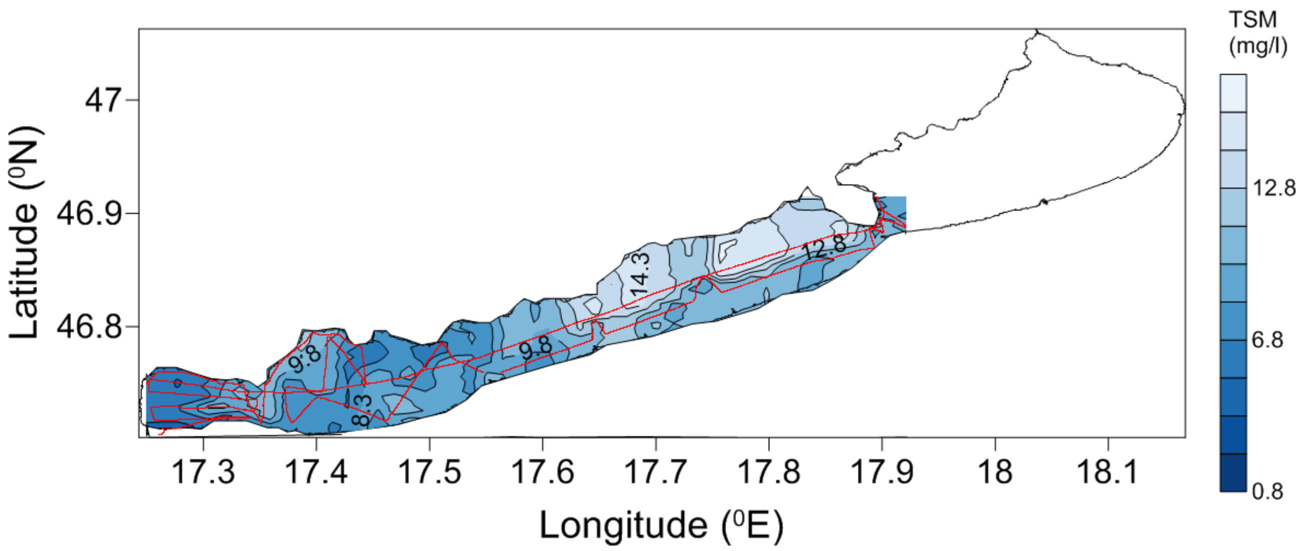

TSM
(mg/l)
12.8
6.8
0.8
47
46.9
46.8
Latitude (0N)
17.3
17.4
17.5
17.6
17.7
17.8
17.9
18
18.1
Longitude (0E)
14.3
12.8
9.8
8.3

River Zala region, mapping a larger scale:

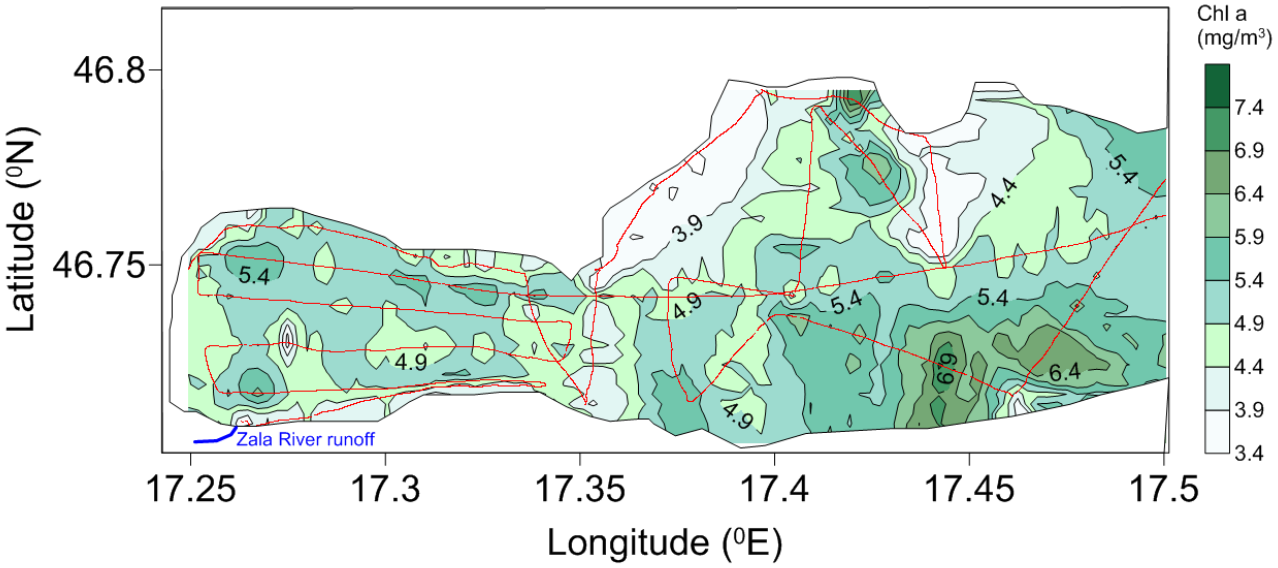

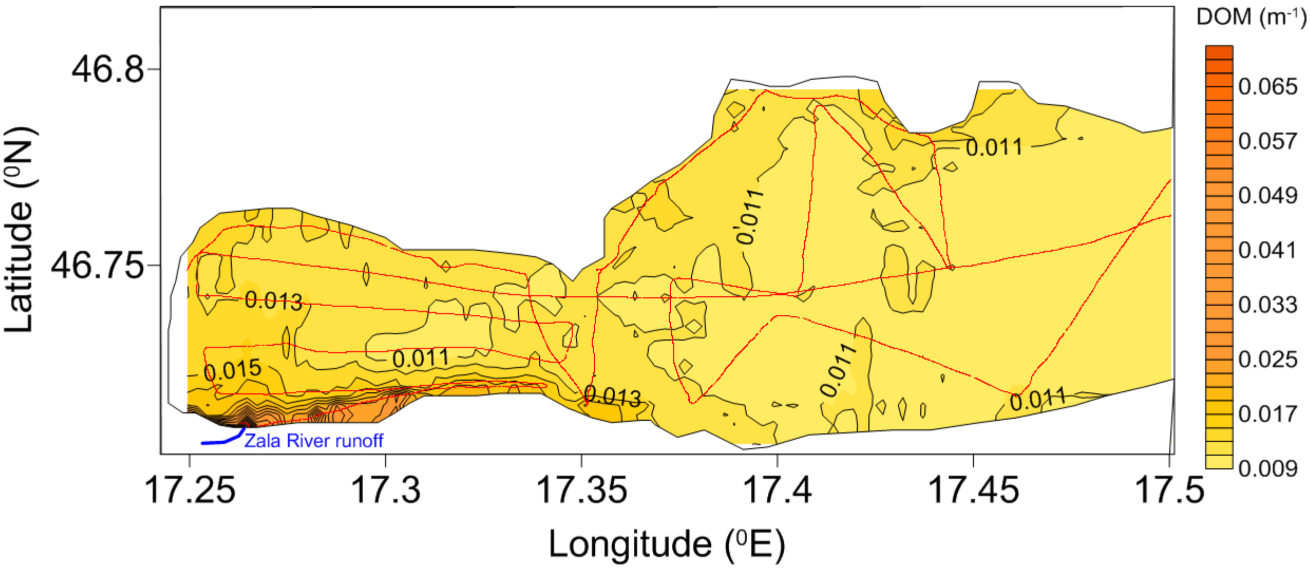

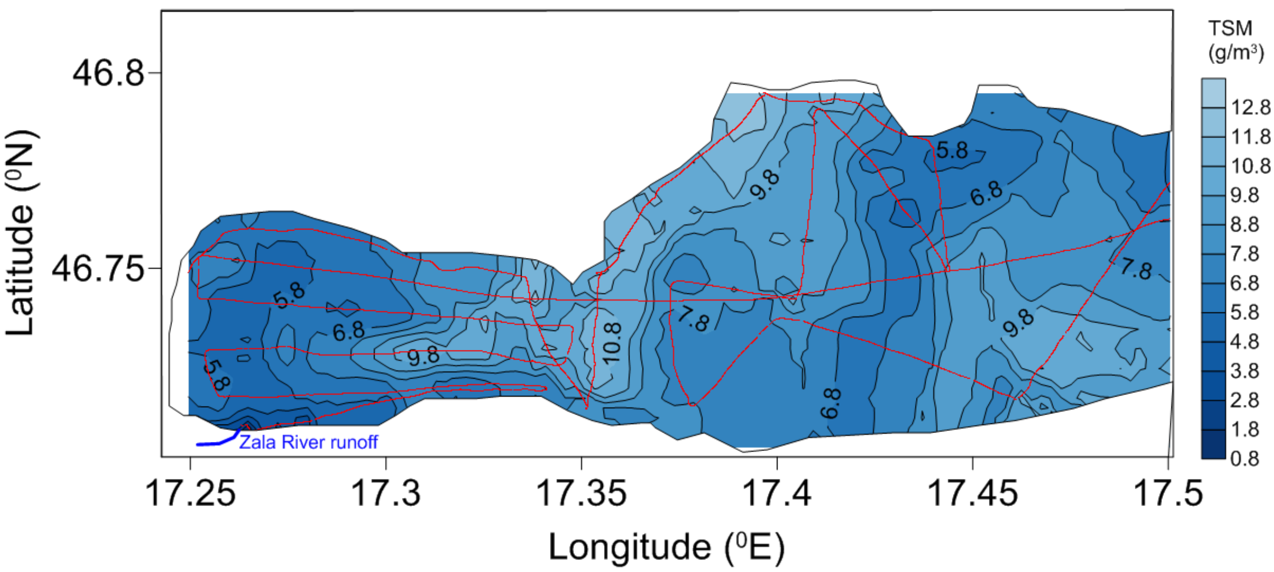

Kis-Balaton Water Retention System created to remove industrial inflows to Lake Balaton (located east of the lake, up the river Zala):

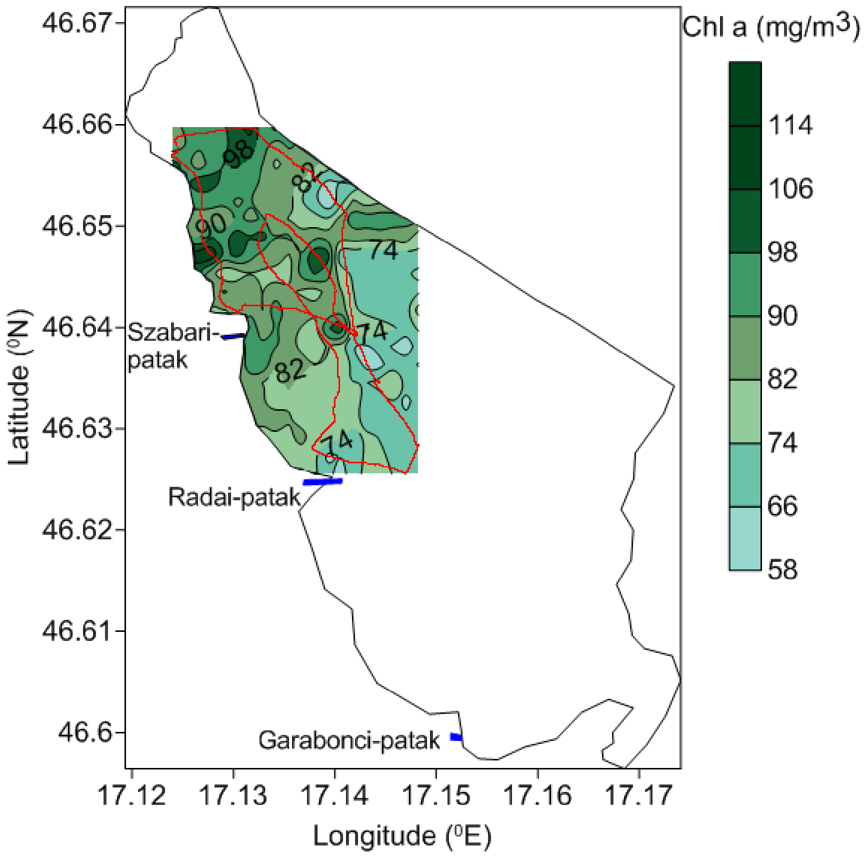

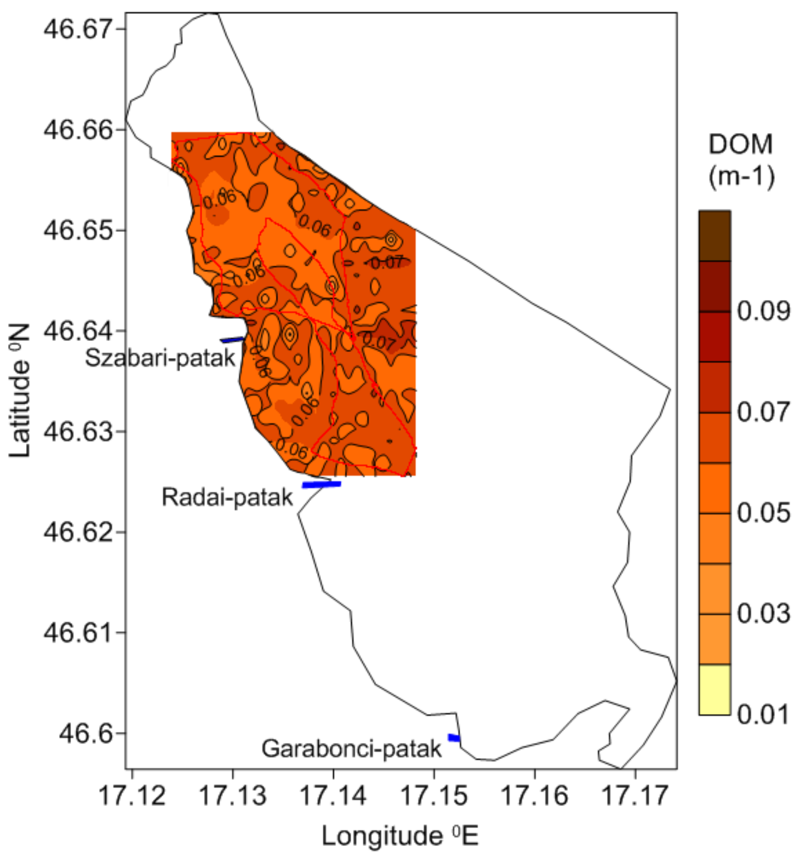

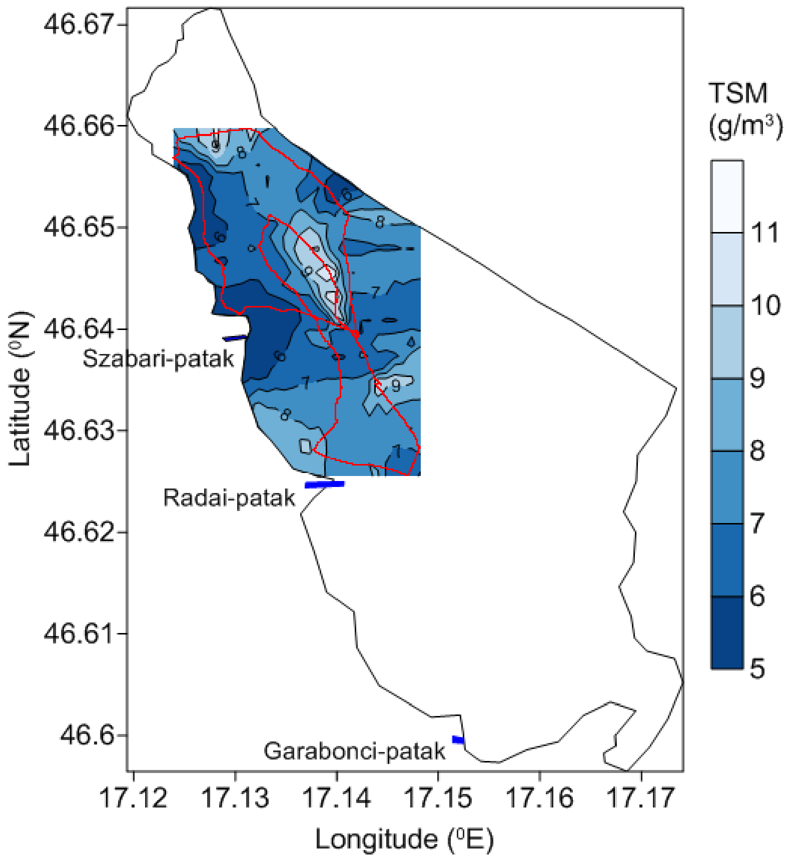

4. Summary

The UV fluorescent LiDARs UFL portable series allows estimating colored dissolved organic matter, oil films and organic (e.g. sewage) pollutants, chlorophyll *a* and mineral suspended matter at very high spatial resolution, distinguishing fine hydrological spatial patterns, in various weather conditions and times of day. The UFL technique gives an opportunity to conduct different kinds of scientific researches and ecological monitoring, collecting great amount of data quickly. However, need to make a calibration of the UFL based on several water samples for laboratory analyses.

The UFL LiDAR observation is an intermediate stage between satellite imaging and water sampling. It is not possible within 1-2 hours to collect a lot of water samples for laboratory analysis in a large area, roughly simultaneous with satellite imaging. Besides, UFL allows collecting data from multiple (tens and hundreds) points within one satellite pixel by crossing it by boat, so after averaging this gives a true mean value for the comparison with the satellite data.

Small-scale spatial variability (patchiness) of chlorophyll a, CDOM and TSM in the upper water layer varies significantly depending on weather conditions, especially wind forcing, also on the type of water body and its currents pattern, and requires further investigation.

References

1. Abramov, O.I.; Eremin, V.I.; Karlsen, G.G.; Lobov, L.I.; Polovinko, V.V. Application of laser ranging to determine the pollution of sea surface by oil products. *Atmos. Ocean. Phys*. **1977**, *13*, 331–334.
2. Aibulatov N.A., Zavialov P.O., Pelevin V.V. Some features of self-purification of Russian Black Sea shoaling waters near river entries // Geo Ecology, **2008**, V.4, 301-310 (in Russian)
3. Babichenko, S.; Dudelzak, A.; Poryvkina, L. Laser remote sensing of coastal and terrestrial pollution by FLS-LIDAR. *EARSeL ePro*. **2004**, *3*, 1–7.
4. Barbini, R.; Colao, F.; Fantoni, R.; Palucci, A.; Ribezzo, S. Shipborne laser remote sensing of the Venice lagoon. *Int. J. Remote Sens*. **1999**, *20*, 2405–2421.
5. Cuthbert, I.D.; del Giorgio, P. Toward a standard method of measuring color in freshwater. Limnol. Oceanogr. **1992**, 37, 1319–1326.
6. Farmer, F.H.; Brown, C.A., Jr.; Jarrett, O., Jr.; Campbell, J.W.; Staton, W.L. Remote Sensing of Phytoplankton Density and Diversity in Narragansett Bay Using an Airborne Fluorosensor. In Proceedings of the 13th International Symposium for Remote Sensing of Environment, Ann Arbor, MI, USA, 23–27 April **1979**.
7. Fiorani, L., Fantoni, R., Lazzara, L., Nardello, I., Okladnikov, I., Palucci, A. Lidar calibration of satellite sensed CDOM in the southern ocean. In Proceedings of the European Association of Remote Sensing Laboratories, **2006**, 5: 89–99.
8. Herodek S. Phytoplankton changes during eutrophication and P and N metabolism. In: Somlyódy L., G. Van Straten (eds.) Modeling and Managing Shallow Lake Eutrophication – With Application to Lake Balaton, **1986**, Springer Verlag 183-203.
9. Hoge, F.E.; Swift, R.N. Airborne simultaneous spectroscopic detection of laser-induced water Raman backscatter and fluorescence from chlorophyll a and other naturally occurring pigment. *Appl. Opt*. **1981**, *20*, 3197–3205.
10. Iwamura, T.; Nagai, H.; Ishimura, S. Improved methods for determining the contents of chlorophyll, protein, ribonucleic and deoxyribonucleic acid in planktonic populations. Int. Rev. ges. Hydrobiol. Hydrogr. **1970**, 55, 131–147.
11. Koprova L.I. Konovalov B.V., Pelevin V.V., Khlebnikov D.V.. Variations in a Set of Optical and Hydrologic Parameters of the Atlantic Surface Waters. // Izvestiya, Atmospheric and Oceanic Physics, **2010**, Vol. 46, No. 2, 192–207.
12. Palmer, S. C. J., T. Kutser, and P. D. Hunter. Remote Sensing of Inland Waters: Challenges, Progress and Future Directions. // Remote Sensing of Environment, **2015**, 157: 1–8. doi:10.1016/j.rse.2014.09.021.
13. Pelevin V.N., Abramov O.I., Karlsen G.G., Pelevin V.V., Stogov A.M., Khlebnikov D.V. Laser sensing of surface water in the Atlantic Ocean and European seas**.** // Atmospheric and oceanic optics. **2001**. V. 14. No. 08. P. 646-650.
14. Presing M., Preston T., Takatsy A., Sprober P., Kovacs A.W., Voros L., Kenesi G. and Kobor I., **2008**. Phytoplankton nitrogen demand and the significance of internal and external nitrogen sources in a large shallow lake (Lake Balaton, Hungary). Hydrobiologia, 599, 87–95

15. Reuter, R., Diebel, D. and Hengstermann, T. Oceanographic laser remote sensing: measurement of hydrographic fronts in the German Bight and in the Northern Adriatic Sea. International Journal of Remote Sensing, **1993**, 14: 823-848.
16. S. Palmer, V. Pelevin, I. Goncharenko, A. Kovács, A. Zlinszky, M. Présing, H. Horváth, V. Nicolás-Perea, Heiko Balzter and Viktor R. Tóth. Ultraviolet Fluorescence LiDAR (UFL) as a Measurement Tool for Water Quality Parameters in Turbid Lake Conditions // Remote Sens. **2013**, 5(9), 4405-4422. http://www.mdpi.com/2072-4292/5/9/4405
17. Utkin, A. B., Lavrov A., Vilar R. Evolution of water pollution by LIF LIDAR. In Proceedings of 31 Symposium of the European Association of Remote Sensing Laboratories, **2011**, 104-113.
18. Zavialov P.O., Kopelevich O.V., Kremenetskiy V.V., Pelevin V.V., Grabovskiy A.B., Gureev B.A., Grigoriev A.V., Peresipkin V.I., Ding C.F., Hsu M.H. A joint Russian-Taiwanese expedition at the shelf of the South China Sea: Searching for manifestations of groundwater discharge to the ocean. // Oceanology, **2010**, Vol. 50, 4, 618-622.
19. Zavialov P.O., Makkaveev P.N., Konovalov B.V., Osadchiev A.A., Khlebopashev P.V., Pelevin V.V., Grabovskiy A.B., Ijitskiy A.A., Goncharenko I.V., Soloviev D.M., Polukhin A.A. Hydrophysical and hydrochemical characteristics of the sea areas adjacent to the mouths of small rivers of the Russian Black Sea coast. // Oceanology, **2014**, V. 54, 3, doi: 10.7868/S0030157414030150
20. Zavialov P.O., Ijitskiy A.A., Osadchiev A.A., Pelevin V.V., Grabovskiy A.B. The structure of thermohaline and bio-optical fields in the surface layer of the Kara Sea in September 2011. // Oceanology, **2015**, Vol. 55, 4, 461-471